

Configurational entropy of ice from thermodynamic integration

Carlos P. Herrero and Rafael Ramírez

Instituto de Ciencia de Materiales de Madrid, Consejo Superior de Investigaciones Científicas (CSIC), Campus de Cantoblanco, 28049 Madrid, Spain

(Dated: June 12, 2021)

The configurational entropy of ice is calculated by thermodynamic integration from high to low temperatures. We use Monte Carlo simulations with a simple energy model which reproduces the Bernal-Fowler ice rules. This procedure is found to be precise enough to give reliable values for the residual entropy s_{th} of different ice phases in the thermodynamic limit. First, we check it for a two-dimensional ice model. Second, we calculate s_{th} for ice Ih, and compare our result with those previously given in the literature. Third, we obtain s_{th} for ice VI, for which we find a value clearly higher than for ice Ih.

I. INTRODUCTION

Water is known to show a wide variety of solid phases, and in fact, sixteen different crystalline ice phases have been identified so far.^{1,2} The determination of their crystal structures and stability range in the pressure-temperature phase diagram has been a matter of research for several decades. However, despite the large amount of experimental and theoretical work on the solid phases of water, some of their properties still lack a complete understanding. This is mainly due to their peculiar structure, where hydrogen bonds between contiguous molecules give rise to properties somewhat different than those of most known liquids and solids.³⁻⁵

In all ice phases (with the exception of ice X), water molecules appear as well defined entities forming a network connected by H-bonds. In this network each water molecule is surrounded by four others in a more or less distorted tetrahedral coordination. The orientation of each molecule with respect to its four nearest neighbors fulfills the so-called Bernal-Fowler ice rules. These rules state that each H₂O molecule is oriented in such a way that its two protons point toward adjacent oxygen atoms and that there must be exactly one proton between two contiguous oxygen atoms.⁶ In the following we will refer to these rules simply as “ice rules.”

The presence of orientational disorder in the water molecules is a property of several ice phases. While the oxygen atoms show a full occupancy (f) of their crystallographic positions, the hydrogen atoms may display a disordered spatial distribution as indicated by a fractional occupancy of their lattice sites. Thus, ice Ih, the stable phase of solid water under normal conditions, presents full proton disorder compatible with the ice rules, i.e., occupancies of H-sites of $f = 0.5$. However, other phases such as ice II are H-ordered, while others as ice III are characterized by a partial proton ordering, i.e., some fractional occupancies of H-sites are different from 0.5.

Configurational disorder of protons in ice was first studied by Pauling,⁷ who estimated its contribution to the entropy of a crystal of N molecules to be $S = Nk_B \ln(3/2)$. This combinatorial estimate turned out to be in good agreement with the “residual” entropy de-

rived from the experimental heat capacity of ice Ih,^{8,9} although the calculation did not take into account the actual structure of ice Ih. Nagle¹⁰ calculated later the residual entropy of hexagonal ice Ih and cubic ice Ic by a series method, and found in both cases very similar values, which turned out to be close to but slightly higher than the Pauling’s estimate. More recently, Berg *et al.*¹¹ have used multicanonical simulations to calculate the configurational entropy of ice Ih, assuming a disordered proton distribution compatible with the ice rules. Moreover, several authors have calculated the configurational entropy of partially ordered ice phases,¹²⁻¹⁴ a question that will not be addressed here.

Ice-type models are important not only for condensed phases of water, but also for other kinds of materials showing atomic disorder,¹⁵ as well as in the statistical mechanics of lattice models.^{16,17} Although exact analytical solutions for the ice model in the actual three-dimensional ice structures are not known at present, an exact solution was found by Lieb for the two-dimensional square lattice.^{18,19} In this case, the configurational entropy results to be $S = Nk_B \ln W$, with $W = (4/3)^{3/2} = 1.5396$, somewhat higher than the Pauling value $W_P = 1.5$.

In this paper, we present a simple, but “formally exact” method, to obtain the configurational entropy of H-disordered ice structures. It is based on a thermodynamic integration from high to low temperatures, for an ice model which reproduces the ice rules at low temperatures.

II. COMPUTATIONAL METHOD

To calculate the configurational entropy of the different ice structures, we consider a simple model. The only requirement for this model is that it has to reproduce the ice rules at low temperature. Thus, irrespective of its simplicity, it can give the actual entropy if an adequate thermodynamic integration is carried out.

For concreteness, we summarize the ice rules:⁶

- (1) There is one hydrogen atom between each pair of neighboring oxygen atoms, forming a hydrogen bond.
- (2) Each oxygen atom is surrounded by four H atoms,

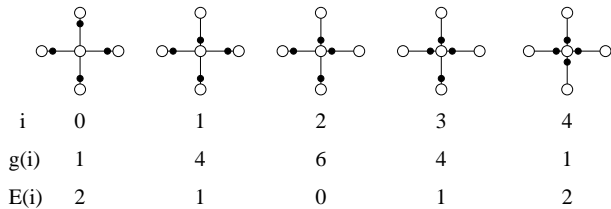


FIG. 1: Sketch of the different hydrogen configurations around an oxygen atom. Open and solid circles represent oxygen and hydrogen atoms, respectively. For each configuration, i is the number of H atoms close to the central oxygen, $g(i)$ indicates its multiplicity, and $E(i)$ refers to its energy in the model described in the text.

two of them covalently bonded and two other H-bonded to it.

Our model is defined as follows. We consider an ice structure as defined by the positions of the oxygen atoms, so that each O atom has four nearest O atoms. This defines a network, where the nodes are the O sites, and the links are H-bonds between nearest neighbors. The network coordination is four, which gives a total of $2N$ links, N being the number of nodes. We assume that on each link there is one (and only one) H atom, which can move between two positions on the link (close to one oxygen or close to the other).

Given a configuration of H atoms on an ice network, the energy U is defined as:

$$U = \sum_{n=1}^N E(i_n) \quad (1)$$

where the sum runs over the N nodes in the network, and i_n is the number of hydrogen atoms covalently bonded to the oxygen on site n , which can take the values 0, 1, 2, 3, or 4. The energy associated to site n is then $E(i_n) = |i_n - 2|$ (see Fig. 1), having a minimum for $i_n = 2$, which imposes the fulfillment of the ice rules at low temperature. In this way, all hydrogen configurations compatible with the ice rules on a given structure are equally probable in the low-temperature limit, i.e., it is implicit in the model that all configurations obeying the ice rules have the same energy.

We note that this simple model, although it is a convenient tool for our present purposes, does not represent any realistic interatomic interaction, in the sense that we are not dealing with a real ordering process, but with a numerical approach to “count” H-disordered configurations of ice. Since the entropy is a state function, one can obtain the number of configurations compatible with the ice rules by a kind of thermodynamic integration from a reference state ($T \rightarrow \infty$) for which the H configuration is random (does not respect the ice rules), to a state in which these rules are strictly fulfilled ($T \rightarrow 0$). We note that in our calculations we use reduced variables, so that all quantities such as the energy U and the temperature T

are dimensionless. The entropy per site s that we calculate is therefore related with the physical configurational entropy S as $S = Nk_B s$.

The heat capacity per site,

$$c_v(T) = \frac{1}{N} \frac{d\langle U \rangle}{dT} \quad (2)$$

has been obtained from the energy fluctuations at temperature T , by using the expression²⁰

$$c_v(T) = \frac{(\Delta U)^2}{NT^2}, \quad (3)$$

where $(\Delta U)^2 = \langle U^2 \rangle - \langle U \rangle^2$. The configurational entropy per site can be obtained from the heat capacity by thermodynamic integration as

$$s(T) = s(\infty) + \int_{\infty}^T \frac{c_v(T')}{T'} dT' \quad (4)$$

In our case, the entropy per site for $T \rightarrow \infty$ is given by

$$s(\infty) = \frac{1}{N} \ln(2^{2N}) = 2 \ln 2 \quad (5)$$

where $2N$ in the exponent indicates the number of links in the network under consideration (Note that 2^{2N} is the total number of possible configurations in our model, since each of the $2N$ links admits two different positions for an H atom).

A practical problem with Eq. (4) in a thermodynamic integration is that the limit $T \rightarrow \infty$ cannot be reached, and any cutoff in the temperature, even if this is taken at large T , can introduce systematic errors in the calculated entropies. To overcome this problem we use the fact that an analytical model can approximate very well the high-temperature thermodynamic variables, with an error smaller than the error bars associated to the simulation procedure. Such an analytical model can be obtained by considering the nodes as “independent”, as in Pauling’s original calculation for a hypothetical network including no loops. In this case, the partition function is given by

$$Z = \frac{z^N}{2^{2N}} \quad (6)$$

where z is the one-site partition function:

$$z = 6 + 8e^{-1/T} + 2e^{-2/T}, \quad (7)$$

(as derived from the Boltzmann factors for 16 possible configurations of four hydrogen atoms; see Fig. 1) and the term 2^{2N} in the denominator appears to avoid counting links with zero or two H atoms. In fact, the high-temperature limit of Z in Eq. (6) is $Z_{\infty} = 16^N/4^N = 2^{2N}$, which is the number of configurations compatible with the condition of having an H atom per link. The energy per site is

$$\langle u \rangle = \frac{4}{z} \left(2e^{-1/T} + e^{-2/T} \right). \quad (8)$$

For the actual ice structures, the corresponding oxygen networks contain loops, which means that the factorization in the partition function in Eq. (6) is not possible. However, at high temperatures thermodynamic variables for the real structures converge to those of the independent-site model. At high temperature, $\langle u \rangle$ in Eq. (8) can be expanded in powers of $1/T$ so that

$$\langle u \rangle = \frac{3}{4} - \frac{7}{16T} + \frac{3}{64T^2} + \frac{19}{768T^3} + \dots \quad (9)$$

and using Eqs. (2) and (4) we find for the entropy

$$s(T) = s(\infty) - \frac{7}{32T^2} + \frac{1}{32T^3} + \frac{19}{1024T^4} + \dots \quad (10)$$

Keeping terms for $s(T)$ up to $1/T^4$, we find $s(T = 10) = 1.38414$. We have checked that at temperatures $T \sim 10$, both the energy and heat capacity derived from this model coincide (within error bars) with those derived from our Monte Carlo simulations for the actual networks studied here. Thus, to obtain the configurational entropy for the ice structures, our thermodynamic integration in fact begins at $T = 10$, a temperature at which the entropy of the actual network is taken as that of the analytical (no loops) model. We note that at lower temperatures ($T \sim 1$), the simulations for the considered networks yield energy values different from those derived from the “independent-node” model in Eqs. (6) and (7), which is in fact the reason why we find for these networks entropy values different from the Pauling result.

With this simple scheme for the energy, we have carried out Monte Carlo simulations on ice networks of different sizes. The largest networks employed here included 3600, 2880, and 3430 sites for the square lattice, ice Ih, and ice VI, respectively. Periodic boundary conditions were assumed. Sampling of the configuration space was carried out by the Metropolis update algorithm.²¹ For each network we considered 360 temperatures in the interval between $T = 10$ and $T = 1$, and 200 temperatures in the range from $T = 1$ to $T = 0.01$. For each considered temperature, the simulation started from the last hydrogen configuration in the previous temperature, and then we carried out 10^4 Monte Carlo steps for system equilibration, followed by 8×10^6 steps for averaging of thermodynamic variables. Each Monte Carlo step consisted of an update of $2N$ (the number of H-bonds) hydrogen positions successively and randomly selected. Finite-size scaling was then employed to obtain the configurational entropy per site s_{th} corresponding to the thermodynamic limit (extrapolation to infinite size).

Using a simple energy model as that employed here, an alternative procedure to calculate the configurational entropy can consist in obtaining directly the density of states as a function of the energy, as described elsewhere for order/disorder problems in condensed matter.²² Then, in our case the entropy could be obtained from the number of states with zero energy, i.e., compatible with the ice rules.

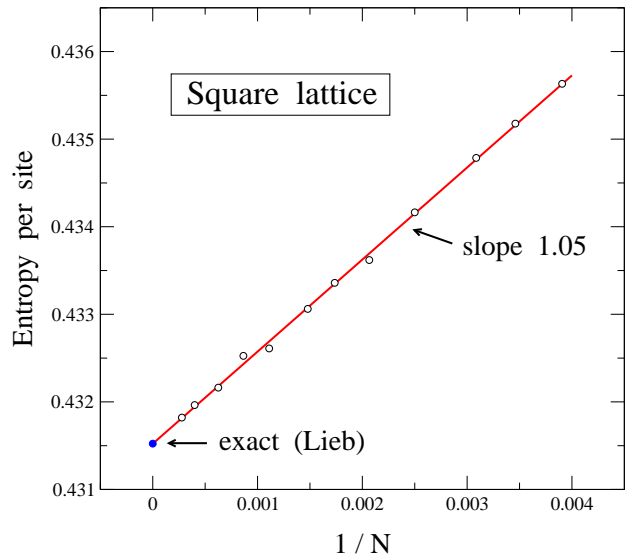


FIG. 2: Entropy per site as a function of the inverse lattice size ($1/N$) for the two-dimensional square lattice. Open circles indicate results of our thermodynamic integration in the limit $T \rightarrow 0$. Error bars are in the order of the symbol size. A solid circle shows the exact analytical result obtained by Lieb.¹⁸

III. RESULTS AND DISCUSSION

We have applied the method described above to calculate the configurational entropy of the ice model in three different networks. First, we check the precision of the method for the two-dimensional square lattice, for which an exact analytical solution is known. Then, we calculate s_{th} for the familiar ice Ih, and compare our results with those obtained in earlier work. Finally, we present results for the configurational entropy of ice VI, for which one expects s_{th} to be appreciably different from ice Ih, due to the presence of four-membered rings of water molecules in its structure.

For each considered network, we have obtained the configurational entropy s_N in the limit $T \rightarrow 0$ for several system sizes N , as described in Sect. II. In Fig. 2 we present s_N for the ice model on the two-dimensional square lattice. Open symbols represent the configurational entropy derived from our thermodynamic integration, as a function of the inverse system size. We find that s_N decreases for increasing system size N , and in fact there is a linear dependence of s_N on $1/N$ for $N \gtrsim 150$, in the form

$$s_N = s_{th} + \frac{a}{N}, \quad (11)$$

where a is a network-dependent parameter. For smaller system sizes (not shown in the figure), s_N deviates slightly from the linear behavior, becoming smaller than the value predicted from a linear fit for $N > 150$ sites. Extrapolation of the linear fit for $1/N \rightarrow 0$ gives a value

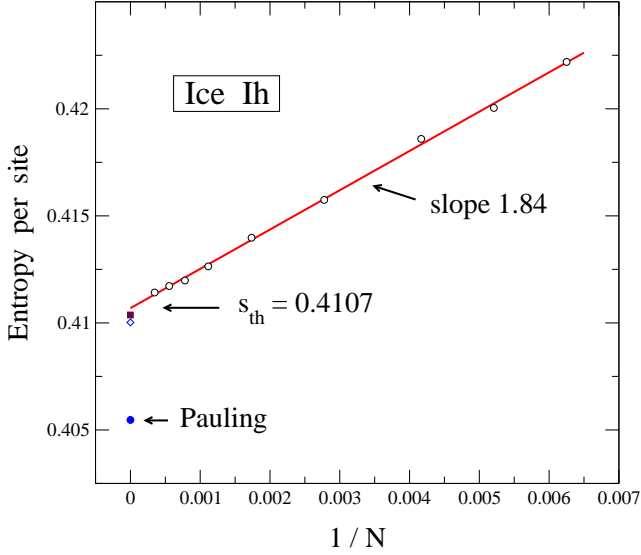


FIG. 3: Entropy per site as a function of the inverse network size ($1/N$) for hexagonal ice Ih. Open circles show results of our thermodynamic integration in the limit $T \rightarrow 0$. Error bars of the data points are on the order of the symbol size. Other symbols represent earlier results for the configurational entropy of ice Ih: solid circle, Pauling⁷; open diamond, Nagle¹⁰; solid square, Berg *et al.*¹¹

$s_{th} = 0.43153(3)$, in good agreement with the exact solution for the square lattice found by Lieb¹⁸ by the transfer-matrix method: $s_{th} = \frac{3}{2} \ln(4/3) = 0.43152$. Information on the least-square fit carried out here is given in Table I.

An argument why the entropy per site should decrease for increasing size is the following. Let us call Ω_N the number of configurations compatible with the ice rules for size N . For two independent cells of size N the number of possible configurations would be Ω_N^2 . Then, putting both cells together to form a larger cell of size $2N$, we have $\Omega_{2N} < \Omega_N^2$, because one has to discard configurations that do not “match” correctly in the border between both N -size cells. The decrease of s_N for increasing N can thus be viewed as an effect of the boundary conditions. Assuming that s_N behaves regularly as a function of $1/N$ in the thermodynamic limit ($1/N \rightarrow 0$), one expects for large N a dependence of the form $s_N = s_{th} + a/N + b/N^2 + \dots$. This is in fact what we find from our simulations, with the parameter b so small that the linear dependence of s_N on $1/N$ is clearly consistent with the results at least for $N > 150$.

For the three-dimensional structure of ice Ih we also find a linear dependence of the configurational entropy on the inverse network size. This is shown in Fig. 3, where one observes that the slope (parameter a in Eq. (11)) is larger than in the case of the two-dimensional lattice. The entropy in the thermodynamic limit is lower for ice Ih, as expected from earlier results for this ice structure.^{10,11} We find $s_{th} = 0.41069(8)$. As already observed in the analytical result by Nagle¹⁰ and in the

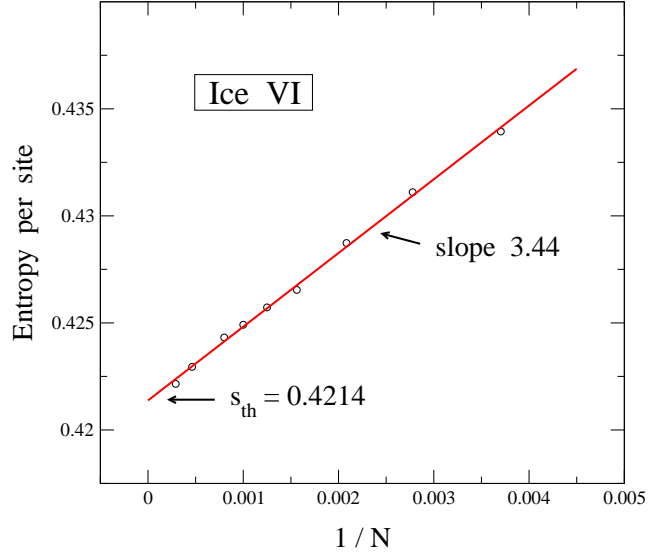


FIG. 4: Entropy per site as a function of the inverse network size ($1/N$) for ice VI. Open circles display results of our thermodynamic-integration procedure in the low-temperature limit. Error bars are in the order of the symbol size.

multicanonical simulations by Berg *et al.*,¹¹ the configurational entropy is higher than the earlier estimate by Pauling. Moreover, our result is slightly higher than that of Nagle¹⁰, who found $s_{th} = 0.41002$. Our result is a little higher than that found by Berg *et al.*,¹¹, although we consider that both data are compatible one with the other, given the error bars (see Table I).

Apart from ice Ih and cubic ice Ic, we are not aware of any direct calculation of the configurational entropy of H-disordered ice for other ice structures. To assess the influence of the ice network on the entropy, we have also considered the case of ice VI, where H atoms are known to be disordered.^{2,4,23} In Fig. 4 we display our results for the configurational entropy of ice VI, as a function of the inverse network size. We find in this case a slope $a = 3.44$, much larger than for the square lattice and ice Ih. The extrapolation of s_N to infinite network size gives $s_{th} = 0.42138(11)$, clearly higher than the value corresponding to ice Ih (a 2.6% larger). This result is remarkable, since up to now the only comparison in this respect concerned ice Ih with the Pauling estimate, being the entropy an 1.3% larger in the former case than in the latter. Now we see that for ice VI the configurational entropy for this H-disordered structure is 3.9% larger than the Pauling result.

We note the tendency of the entropy s_{th} to increase due to the presence of loops in the ice structure. In fact, the Pauling approximation neglects the presence of loops, as happens in the so-called Bethe lattice (also known as Cayley tree).^{16,17} This gives a value $s_{th} = 0.40547$. For ice Ih, which contains six-membered rings of water molecules, the entropy is higher by an 1.3%, and it is still higher for the square lattice with four-membered rings (a

TABLE I: Entropy for the ice model on the square lattice, ice Ih, and ice VI, as derived from our Monte Carlo simulations. n_P : number of data points employed in the linear fits; a : slope of the linear fit as in Eq. (11); ρ : correlation coefficient. For comparison, we give the entropy values obtained in earlier works.

Ice	Author	n_P	a	s_{th}	W	ρ
Square	This work	12	1.05(1)	0.43153(3)	1.53961(5)	0.9994
Square	Lieb ¹⁸			0.431523	1.539601	
Ih	This work	9	1.84(2)	0.41069(8)	1.50786(12)	0.9994
Ih	Nagle ¹⁰			0.41002(10)	1.50685(15)	
Ih	Berg <i>et al.</i> ¹¹			0.4104(2)	1.5074(3)	
VI	This work	9	3.44(6)	0.42138(11)	1.52406(16)	0.9990
Generic	Pauling ⁷			0.405465	1.5	

6.4% respect the Pauling approach). With this trend in mind, we could expect for ice VI a value of the entropy intermediate between those of ice Ih and the square lattice, as it contains four- and six-membered rings (apart from other larger loops).^{4,24,25} Similarly, for ice networks with larger ring sizes, one can expect a smaller configurational entropy for disordered hydrogen distributions, and thus closer to the Pauling result.

Some further comments on Table I are in order. In most papers dealing with the configurational entropy of ice, it is the parameter W which is given, instead of the entropy s_{th} itself. As we find directly s_{th} from our thermodynamic integration, we have calculated W in the different cases as $W = \exp(s_{th})$. Also the error bars ΔW and Δs_{th} in the values of s_{th} and W , respectively, are related by the expression $\Delta W = W \Delta s_{th}$, as can be derived by differentiating the exponential function. Our error bars for s_{th} represent one standard deviation, as given by the least-square procedure employed to fit the data. In the result by Nagle,¹⁰ the error bar was estimated by this author from an extrapolation of the series terms calculated in his analytical procedure. Note also that, although the result obtained by Pauling was intended to reproduce the residual entropy of ice Ih, it does not take into account the actual ice network, but only the four-fold coordination of the structure. For this reason we qualify it as “generic”. Concerning the results by Berg *et al.*¹¹, we note that these authors have recently²⁶ given an entropy value for ice Ih slightly smaller than their earlier result, but both of them are compatible one with the other, taking into account the statistical error bars.

To avoid any possible confusion, we emphasize that the simple model employed in our calculations is not intended

to reproduce any physical characteristic of ice (such as order/disorder transitions) further than calculating the entropy of an H distribution compatible with the ice rules. It implicitly assumes that the distribution of H atoms on the ice network has no long-range order, and only imposes strict fulfillment of the ice rules (short-range order) in the limit $T \rightarrow 0$. The configurational entropy obtained in this way is what has been traditionally called residual entropy of ice.⁷ With this in mind, we are not allowing for any violation of the third law of Thermodynamics.

In this context, it is generally accepted that the equilibrium ice phases in the low-temperature limit (at low and high pressures) display ordered proton structures, as expected from a vanishing of the entropy. Order-disorder transitions have been observed between several pairs of ice phases.^{1,2,25} These transitions are accompanied by orientational ordering of the water molecules, which implies a kinetically unfavorable reorganization of the H-bond network. In several cases, the transition from a disordered to an ordered phase only occurs after doping the sample, which seems to provide a mechanism favoring the rearrangement of the H-bond network.^{25,27,28} Thus, at low temperature ice Ih transforms into ice XI, an H-ordered phase, but this transition has never been observed in pure ice, only in doped materials at 72 K.^{27–29} Something similar happens for high-pressure phases, and ice VI in particular transforms into proton-ordered ice XV.^{2,24}

Given the entropy difference found here for real structures such as ice Ih and ice VI, a detailed knowledge of the configurational entropy for the different ice phases can be important for precise calculations of the phase diagram of water,^{30,31} as noted earlier for ice phases with

partial proton ordering.¹³

IV. CONCLUSIONS

We have presented results for the configurational entropy of H-disordered ice structures, calculated by means of a thermodynamic integration. A simple model allowed us to derive the entropy corresponding to each structure. This procedure has turned out to be very precise, indicating that the associated error bars can be made very small without employing sophisticated methods, but only using standard statistical mechanics and numerical procedures.

For real ice structures, such as ice Ih and ice VI, we find a difference in configurational entropy of 2.6%. For

ice VI we obtain an entropy value 3.9% higher than the Pauling estimate, as a consequence of its particular network connectivity. This method can be applied to other ice structures with hydrogen disorder, which will presumably give different values for the configurational entropy, due to differences in their network topology.

Acknowledgments

This work was supported by Dirección General de Investigación Científica y Técnica (Spain) through Grant FIS2012-31713 and by Comunidad Autónoma de Madrid through Program MODELICO-CM/S2009ESP-1691.

-
- ¹ A. N. Dunaeva, D. V. Antsyshkin, and O. L. Kuskov, *Solar System Research* **44**, 202 (2010).
 - ² T. Bartels-Rausch, V. Bergeron, J. H. E. Cartwright, R. Escribano, J. L. Finney, H. Grothe, P. J. Gutierrez, J. Haapala, W. F. Kuhs, J. B. C. Pettersson, et al., *Rev. Mod. Phys.* **84**, 885 (2012).
 - ³ D. Eisenberg and W. Kauzmann, *The Structure and Properties of Water* (Oxford University Press, New York, 1969).
 - ⁴ V. F. Petrenko and R. W. Whitworth, *Physics of Ice* (Oxford University Press, New York, 1999).
 - ⁵ G. W. Robinson, S. B. Zhu, S. Singh, and M. W. Evans, *Water in Biology, Chemistry and Physics* (World Scientific, Singapore, 1996).
 - ⁶ J. D. Bernal and R. H. Fowler, *J. Chem. Phys.* **1**, 515 (1933).
 - ⁷ L. Pauling, *J. Am. Chem. Soc.* **57**, 2680 (1935).
 - ⁸ W. F. Giauque and J. W. Stout, *J. Amer. Chem. Soc.* **58**, 1144 (1936).
 - ⁹ O. Haida, T. Matsuo, H. Suga, and S. Seki, *J. Chem. Thermodyn.* **6**, 815 (1974).
 - ¹⁰ J. F. Nagle, *J. Math. Phys.* **7**, 1484 (1966).
 - ¹¹ B. A. Berg, C. Muguruma, and Y. Okamoto, *Phys. Rev. B* **75**, 092202 (2007).
 - ¹² R. Howe and R. W. Whitworth, *J. Chem. Phys.* **86**, 6443 (1987).
 - ¹³ L. G. MacDowell, E. Sanz, C. Vega, and J. L. F. Abascal, *J. Chem. Phys.* **121**, 10145 (2004).
 - ¹⁴ B. A. Berg and W. Yang, *J. Chem. Phys.* **127**, 224502 (2007).
 - ¹⁵ S. V. Isakov, K. S. Raman, R. Moessner, and S. L. Sondhi, *Phys. Rev. B* **70**, 104418 (2004).
 - ¹⁶ J. M. Ziman, *Models of disorder* (Cambridge University, Cambridge, 1979).
 - ¹⁷ G. M. Bell and D. A. Lavis, *Statistical Mechanics of Lattice Models. Volume 1: Closed Form and Exact Theories of Cooperative Phenomena* (Ellis Horwood Ltd., New York, 1989).
 - ¹⁸ E. H. Lieb, *Phys. Rev. Lett.* **18**, 692 (1967).
 - ¹⁹ E. H. Lieb, *Phys. Rev.* **162**, 162 (1967).
 - ²⁰ D. Chandler, *Introduction to modern statistical mechanics* (Oxford University Press, Oxford, 1987).
 - ²¹ K. Binder and D. W. Heermann, *Monte Carlo Simulation in Statistical Physics* (Springer, Berlin, 1997), 3rd ed.
 - ²² C. P. Herrero and R. Ramírez, *Chem. Phys. Lett.* **194**, 79 (1992).
 - ²³ W. F. Kuhs, J. L. Finney, C. Vettier, and D. V. Bliss, *J. Chem. Phys.* **81**, 3612 (1984).
 - ²⁴ C. G. Salzmann, P. G. Radaelli, S. B. and F. J. L., *Phys. Chem. Chem. Phys.* **13**, 18468 (2011).
 - ²⁵ S. J. Singer and C. Knight, *Adv. Chem. Phys.* **147**, 1 (2012).
 - ²⁶ B. A. Berg, C. Muguruma, and Y. Okamoto, *Mol. Sim.* **38**, 856 (2012).
 - ²⁷ A. J. Leadbetter, R. C. Ward, J. W. Clark, P. A. Tucker, T. Matsuo, , and H. Suga, *J. Chem. Phys.* **82**, 424 (1985).
 - ²⁸ C. M. B. Line and R. W. Whitworth, *J. Chem. Phys.* **104**, 10008 (1996).
 - ²⁹ R. Howe and R. W. Whitworth, *J. Chem. Phys.* **90**, 4450 (1989).
 - ³⁰ E. Sanz, C. Vega, J. L. F. Abascal, and L. G. MacDowell, *Phys. Rev. Lett.* **92**, 255701 (2004).
 - ³¹ R. Ramírez, N. Neuerburg, and C. P. Herrero, *J. Chem. Phys.* **137**, 134503 (2012).